SIAM J. MATH. ANAL.
Vol. 46, No. 4, pp. 2743–2766
© 2014 Society for Industrial and Applied Mathematics

Downloaded 09/19/14 to 129.25.6.190. Redistribution subject to SIAM license or copyright; see http://www.siam.org/journals/ojsa.php

THE NONLINEAR HEAT EQUATION ON DENSE GRAPHS AND GRAPH LIMITS*

GEORGI S. MEDVEDEV†

Abstract. The continuum limit of coupled dynamical systems is an approximate procedure, by which the dynamical problem on a sequence of large graphs is replaced by an evolution integral equation on a continuous spatial domain. While this method has been widely used in the analysis of pattern formation in nonlocally coupled networks, its mathematical basis remained little understood. In this paper, we use the combination of ideas and results from the theory of graph limits and nonlinear evolution equations to provide a rigorous mathematical justification for taking the continuum limit and to extend this method to cover many complex networks, for which it has not been applied before. Specifically, for dynamical networks on convergent sequences of simple and weighted graphs, we prove convergence of solutions of the initial-value problems for discrete models to those of the limiting continuous equations. In addition, for sequences of simple graphs converging to {0, 1}-valued graphons, it is shown that the convergence rate depends on the fractal dimension of the boundary of the support of the graph limit. These results are then used to study the coexistence of coherence and incoherence in chimera states and the attractors of the nonlocal Kuramoto equation on certain multipartite graphs. Furthermore, the analytical tools developed in this work are used in the rigorous justification of the continuum limit for networks on random graphs that we undertake in a companion paper [*Arch. Ration. Mech. Anal.*, 21 (2014), pp. 781–803]. As a by-product of the analysis of the continuum limit on deterministic and random graphs, we identify the link between this problem and the convergence analysis of several classical numerical schemes: the collocation, Galerkin, and Monte Carlo methods. Therefore, our results can be used to characterize convergence of these approximate methods of solving initial-value problems for nonlinear evolution equations with nonlocal interactions.

Key words. dynamical network, graph limit, continuum limit

AMS subject classifications. 34C15, 45J05, 45L05, 05C90

DOI. 10.1137/130943741

1. Introduction.

Coupled dynamical systems on graphs represent many diverse models throughout the natural sciences and technology. Examples range from regulatory and neuronal networks in biology [21, 5, 31, 41], to Josephson junctions and coupled lasers in physics [24, 36, 44], to communication, sensor, and power networks in technology [13, 28], to name a few. Compared to partial differential equations and lattice dynamical systems, the analysis of networks meets a new principal challenge: the rich variety and possible complexity of the underlying graphs. The algebraic methods of the graph theory [6, 11] have been useful in understanding the contribution of the network topology to certain aspects of networks dynamics, especially in problems involving synchronization [28, 31]. The continuum limit of nonlocally coupled dynamical networks is one of few analytical approaches that have a potential for elucidating dynamics of a broad class of networks [19, 1, 46, 17, 34, 32, 2]. In this limit, the solutions of the initial-value problems (IVPs) for evolution equations on large discrete networks are approximated by those for the limiting integro-differential equations posed on continuous spatial domains. This limiting procedure has been used to study the mechanisms of some very interesting effects such as chimera states [19, 1],

*Received by the editors November 1, 2013; accepted for publication (in revised form) May 9, 2014; published electronically July 29, 2014. This work was supported in part by the NSF grant DMS 1109367.

http://www.siam.org/journals/sima/46-4/94374.html

†Department of Mathematics, Drexel University, Philadelphia, PA 19104 (medvedev@drexel.edu).

Copyright © by SIAM. Unauthorized reproduction of this article is prohibited.

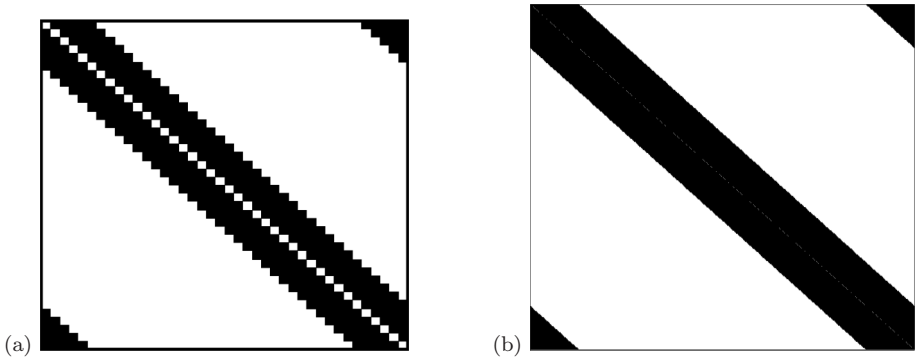

FIG. 1. *The plot of the support of the function W_{G_n} representing the adjacency matrix of the k-nearest-neighbor graph G_n* (a) *and that of its limit W_G* (b). *Both functions are defined on the unit square I^2 and are equal to* 1 *on black cells and* 0 *otherwise.*

multistability [46, 17], synchronization, and the coherence-incoherence transition [34]. However, a rigorous justification for taking the continuum limit in nonlocally coupled models was lacking. In this paper, we use the combination of techniques from the theory of evolution equations [14] and the recent theory of graph limits [9, 8, 26, 27, 25] to provide such justification for a large class of dynamical models on deterministic graphs. In [29], we extend this approach to justify the continuum limit for networks on W-random graphs [25, 26]. The latter include many random graphs that are important in applications, such as Erdős–Rényi and small-world graphs [3, 4, 30, 45].

To motivate the forthcoming analysis of the continuum limit in the nonlocally coupled systems, we first review a representative example. In [46], Wiley, Strogatz, and Girvan studied a nonlocally coupled system of Kuramoto oscillators

$$\dot{\phi}_i = \omega + \frac{1}{n}\sum_{j=i-k}^{i+k} \sin\left(\phi_j - \phi_i\right), \tag{1.1}$$

where $\phi_i : \mathbb{R}^+ \to \mathbb{S}^1 := \mathbb{R}/2\pi\mathbb{Z}$, $i \in [n] := \{1, 2, 3, \dots, n\}$, is interpreted as the phase of oscillator i, ω is the intrinsic frequency, and the sum models the interactions between oscillator i and k of its nearest neighbors from each side (cf. [18, 19]). The oscillators are located on a ring and indexed by integers from $\mathbb{Z}/n\mathbb{Z}$. By recasting (1.1) in a uniformly rotating frame of reference, one can absorb ω. Thus, below we set $\omega = 0$.

It is instructive to view (1.1) as a system of differential equations on graph $G_n = \langle V(G_n), E(G_n)\rangle$ with the vertex set $V(G_n) = [n]$ and the edge set

$$E(G_n) = \left\{(i,j) \in [n]^2 :\ 0 < \operatorname{dist}(i,j) \le k\right\}, \text{ where } \operatorname{dist}(i,j) = \min\{|i-j|, n-|i-j|\}.$$

Let $W_{G_n} :\ I^2 \to \{0,1\}$ such that

$$W_{G_n}(x,y) = 1 \text{ if } (i,j) \in E(G_n) \text{ and } (x,y) \in [(i-1)n^{-1}, in^{-1}) \times [(j-1)n^{-1}, jn^{-1}).$$

Here and below, I denotes $[0,1]$, the spatial domain of the continuum limits considered in this paper. The plot of the support of $W_{G_n}(x,y)$ in Figure 1(a) provides the pixel picture of the adjacency matrix of G_n [6]. In Figure 1(a) and in similar plots throughout this paper, we place the origin in the top left corner of the plot to emphasize the correspondence between W_{G_n} and the adjacency matrix of G_n. As $n \to \infty$,

Copyright © by SIAM. Unauthorized reproduction of this article is prohibited.

Downloaded 09/19/14 to 129.25.6.190. Redistribution subject to SIAM license or copyright; see http://www.siam.org/journals/ojsa.php

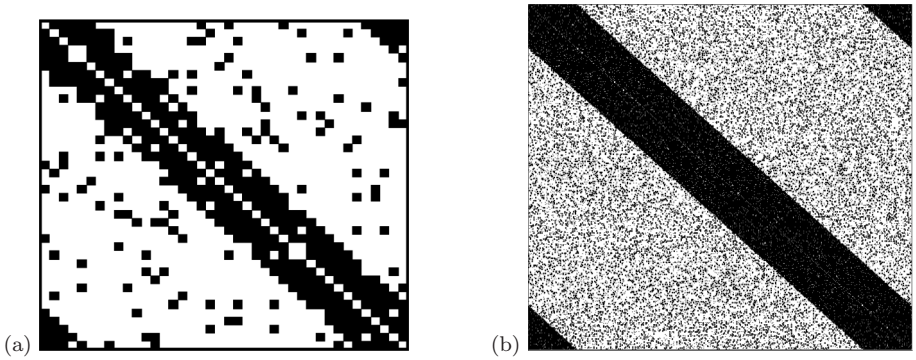

FIG. 2. (a) *The pixel picture of a small-world graph obtained from that shown in Figure* 1(a) *by replacing a random set of the local connections by randomly chosen long-range ones.* (b) *The pixel picture for a large small-world graph.*

$\{W_{G_n}\}$ converges to the $\{0,1\}$-valued function $W_G(x,y)$, whose support is shown in Figure 1(b).

In [46], the analysis of the attractors of (1.1) employs the continuum limit of (1.1). Specifically, let $k = rn$ for some fixed $r \in (0,1]$. After interpreting the right-hand side of (1.1) as a Riemann sum and sending $n \to \infty$, in the uniformly rotating frame of coordinates (1.1) formally becomes

$$\frac{\partial}{\partial t}\phi(x,t) = \int_I W_G(x,y)\sin\left(\phi(y,t) - \phi(x,t)\right) dy, \tag{1.2}$$

where $\phi(x,t)$ describes the evolution of the continuum of oscillators distributed over I. Equation (1.2) is called the continuum (thermodynamic) limit of (1.1).[1]

The continuum equation (1.2) has a family of steady state solutions

$$\theta^{(q)}(x,t) = 2\pi q x + c,\ q \in \mathbb{Z},\ c \in \mathbb{R}, \tag{1.3}$$

called q-twisted states. In [46], the stability analysis of the continuous twisted states (1.3) was used to study their discrete counterparts, which are the steady state solutions of (1.1) ($\omega = 0$) for finite n. The stability analysis in [46] can, in fact, be completely translated into the discrete setting. However, suppose we replace the family of k-nearest-neighbor graphs in (1.1) by a family of small-world graphs (see Figure 2(a)). Then not only does the continuum limit provide a convenient setting for the stability analysis but also the twisted states, as the steady states of the Kuramoto model, exist only in the limit as the number of oscillators goes to infinity (see Figure 2(b)) [30]. Therefore, in this case the continuum limit affords the analysis of the asymptotic behavior of solutions of the Kuramoto model for large n, which is not otherwise feasible in the discrete setting. The Kuramoto–Battogtokh model generating chimera states [19] is another example, where the continuum limit seems to be critical for understanding the nontrivial dynamics in the discrete systems. We will return to the discussion of chimera states in section 6.1.

[1] There is another form of the continuum limit for the Kuramoto model [39, 40, 35, 20]. It is formulated in terms of the density characterizing the state of the continuous system. We do not consider this limit in the present paper.

Copyright © by SIAM. Unauthorized reproduction of this article is prohibited.

Downloaded 09/19/14 to 129.25.6.190. Redistribution subject to SIAM license or copyright; see http://www.siam.org/journals/ojsa.php

Downloaded 09/19/14 to 129.25.6.190. Redistribution subject to SIAM license or copyright; see http://www.siam.org/journals/ojsa.php

These examples lead to the following questions.

(A) Does the continuum model (1.2) truly approximate the dynamics of the discrete model (1.1) for large finite n? If so, in what sense do the solutions of the integro-differential equation approximate those of (1.1) with $\omega = 0$?

(B) How big is the class of network topologies for which one can use the continuum limit? Is it restricted to the special graphs like k-nearest-neighbor on a ring? Can it be applied, for instance, to the small world networks, the original motivation for the analysis in [46]?

The function W_G shown in Figure 1(b) is the limit of the functions $\{W_{G_n}\}$ (Figure 1(a)) representing the adjacency matrices of the k-nearest neighbor family of graphs $\{G_n\}$. The latter is an example of a convergent graph sequence and W_G is the corresponding graph limit [25]. We will explain the meaning of the limit of a graph sequence in section 2. Meanwhile, we refer to the geometric interpretation of the adjacency matrix for the k-nearest-neighbor graph in Figure 1(a), which suggests the limiting pattern of $\{W_{G_n}\}$ as $n \to \infty$ (see Figure 1(b)). Likewise, the pixel picture of the large small-world graph in Figure 2(b) suggests the (piecewise constant) limit for the small-world family of graphs, which in turn can be used in the derivation of the continuum model like (1.2) [30]. These observations hint at the possible relevance of the theory of graph limits for constructing the continuum limits for dynamical networks. We explore this relation for dynamical systems on convergent families of deterministic graphs in this paper and extend this approach to random networks in [29]. Interestingly, in the process of justifying the continuum limit, we discovered the link between this problem and that of convergence of several classical numerical methods. Specifically, we show that dynamical networks on simple and weighted graphs analyzed in sections 4 and 5 can be interpreted as the discretizations of the continuum evolution equation by the collocation method and the Galerkin method, respectively. Furthermore, the analysis of the continuum limit for networks on random graphs in [29] features a similar connection with the Monte Carlo method. Therefore, in addition to the rigorous justification of taking the continuum limit for a large class of dynamical networks, our results characterize convergence of these numerical methods for solving IVPs for certain nonlinear integro-differential equations.

This paper is organized as follows. We review the necessary background on graph limits in section 2. In section 3, we discuss the heat equation on graphs and graph limits. Here, we extend a classical linear heat equation on graphs to allow nonlinear diffusion. This extension covers many dynamical networks arising in applications including coupled oscillator models like (1.1). In the same section, we formally define the continuum limit for dynamical networks of a convergent sequence of dense (weighted) graphs. In this limit, the discrete diffusion operator becomes an integral operator with the kernel representing the limit of the infinite family of graphs. We show that the IVP for the limiting equation is well-posed and admits a unique solution in $C^1(\mathbb{R}; L^\infty(I))$. Further, in Theorem 3.3, we specify assumptions on the kernel and the initial conditions, which guarantee that the solutions of the IVPs remain continuous in space over subdomains of I. This result is used to characterize the attractors of the continuum model. In particular, we apply it to study the coexistence of coherence and incoherence in chimera states and attractors of the Kuramoto equation on certain multipartite graphs (see section 6). The rest of the paper is focused on studying the relation between the solutions of the IVPs for discrete networks and their continuum counterparts. In section 4, for sequences of simple graphs converging to $\{0, 1\}$-valued graphons, we show that the rate of convergence depends on the fractal dimension of the boundary of the support of the graph limit. This shows explicitly how the

Copyright © by SIAM. Unauthorized reproduction of this article is prohibited.

Downloaded 09/19/14 to 129.25.6.190. Redistribution subject to SIAM license or copyright; see http://www.siam.org/journals/ojsa.php

geometry of the graphon affects the accuracy of the continuum limit. In section 5, we analyze networks on convergent weighted graph sequences. The results of this paper are illustrated with the discussion of the dynamics of two concrete models: the Kuramoto–Battogtokh nonlocal system generating chimera states [19] and the Kuramoto equation on multipartite graphs (cf. section 6). The final section, section 7, contains concluding remarks.

2. Graph limits. In this section, we review several definitions and results from the theory of graph limits that we will need later. In our brief tour through graph limits, we mainly follow [7]. For the full exposition of this powerful theory with many diverse applications, we refer an interested reader to the pioneering papers by Lovász and Szegedy [26, 27] and Borgs and others [9, 8] (see also [37]), and to the monograph [25].

It is instructive to start with unweighted simple graphs. We will deal with weighted networks in section 5. An undirected graph $G = \langle V(G), E(G)\rangle$ without loops and multiple edges is called simple. $V(G)$ stands for the set of nodes, and $E(G) \subset V(G) \times V(G)$ denotes the edge set.

Let $G_n = \langle V(G_n), E(G_n)\rangle, n \in \mathbb{N}$, be a sequence of dense finite simple graphs, i.e., $|E(G_n)| = O(|V(G_n)|^2)$, where $|\cdot|$ denotes the cardinality of a set. The convergence of the graph sequence $\{G_n\}$ is defined in terms of the homomorphism densities

$$t(F, G_n) = \frac{\hom(F, G_n)}{|V(G_n)|^{|V(F)|}}. \tag{2.1}$$

Here, $F = \langle V(F), E(F)\rangle$ is a simple graph and $\hom(F, G_n)$ stands for the number of homomorphisms (i.e., adjacency preserving maps $V(F) \to V(G_n)$). In probabilistic terms, (2.1) is the likelihood of a random map $h : V(F) \to V(G_n)$ to be a homomorphism.

Definition 2.1 (see [26, 8]). *The sequence of graphs $\{G_n\}$ is called convergent if $t(F, G_n)$ is convergent for every simple graph F.*[2]

It turns out that the limiting object can be represented by a measurable symmetric function $W : I^2 \to I$. We recall that I stands for $[0, 1]$. Such functions are called graphons. The set of all graphons is denoted by $\mathcal{W}_0$.

Theorem 2.2 (see [26]). *For every convergent sequence of simple graphs, there is $W \in \mathcal{W}_0$ such that*

$$t(F, G_n) \to t(F, W) := \int_{I^{|V(F)|}} \prod_{(i,j)\in E(F)} W(x_i, x_j)dx \tag{2.2}$$

for every simple graph F. Moreover, for every $W \in \mathcal{W}_0$ there is a sequence of graphs $\{G_n\}$ satisfying (2.2).

Graphon W in (2.2) is the limit of the convergent sequence $\{G_n\}$. It is unique up to measure preserving transformations in the sense that for any other limit $W' \in \mathcal{W}_0$ there are measure preserving maps $\phi, \psi : I \to I$ such that $W(\phi(x), \phi(y)) = W'(\psi(x), \psi(y))$ [7, Theorem 2.1]. Geometrically, graphon W representing the limit of

[2]Note that $t(F, G_n) = o(1)$ if $|E(G_n)| = o(|V(G_n)|^2)$, i.e., this definition is meaningful only for sequences of dense graphs. For approaches to convergence of sequences of graphs of bounded degree, we refer the reader to [25]. In the theory of graph limits, convergence in Definition 2.1 is called left-convergence. Since this is the only convergence of graph sequences used in this paper, we refer to the left-convergent sequences as convergent.

Copyright © by SIAM. Unauthorized reproduction of this article is prohibited.

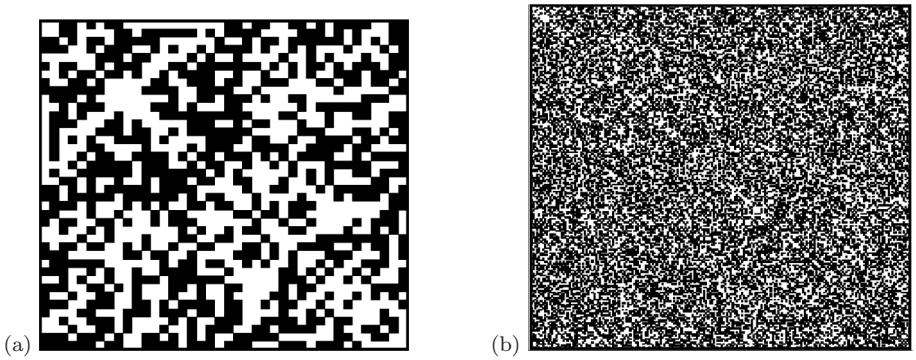

FIG. 3. (a) *The pixel picture of the Erdős–Rényi graph* $G(40, 0.5)$. *The edge between a pair of distinct nodes is inserted with probability* 0.5. (b) *The pixel picture of* $G(600, 0.5)$.

a convergent sequence of simple graphs $\{G_n\}$ can be interpreted as the limit of

$$W_{G_n}(x,y) = \begin{cases} 1 & \text{if } (i,j) \in E(G_n) \text{ and } (x,y) \in \left[\frac{i-1}{n}, \frac{i}{n}\right) \times \left[\frac{j-1}{n}, \frac{j}{n}\right), \\ 0 & \text{otherwise.} \end{cases} \tag{2.3}$$

The support of W_{G_n} provides the pixel picture of the adjacency matrix of G_n (see, e.g., Figure 1(a)). After relabeling the nodes of $\{G_n\}$, if necessary, $\{W_{G_n}\}$ converges to W in the cut-norm [7, Theorem 2.3]. The latter is defined for $W \in L^1(I^2)$ by

$$\|W\|_\square = \sup_{S,T \in \mathcal{L}_I} \left| \int_{S \times T} W(x,y) dx dy \right|,$$

where $\mathcal{L}_I$ stands for the set of all Lebesgue measurable subsets of I. Since for any $W \in L^1(I^2)$

$$\|W\|_\square \le \|W\|_{L^1(I^2)},$$

convergence of $\{W_{G_n}\}$ in the L^1-norm implies convergence of the graph sequence $\{G_n\}$. The deterministic networks analyzed in this paper are convergent with respect to the stronger L^1-norm. The convergence of graphons with respect to the cut-norm does not in general imply that with respect to L^1-norm. For instance, the sequence of Erdős–Rényi graphs with edge density $p \in (0,1)$ is convergent to the constant function p on I^2, Const(p) [26, 8], while no sequence of $\{0,1\}$-valued graphons can converge to Const(p) with $p \in (0,1)$ in the L^1-norm. In particular, L^1-estimates for graphons are insufficient for the analysis of the continuum limits of networks on random graphs [29].

We conclude this section with two examples of convergent graph sequences.

Example 2.3 (see [26, 8]). The Erdős–Rényi graphs. Let $p \in (0,1)$ and consider a sequence of random graphs $G(n,p) = \langle V(G(n,p)), E(G(n,p)) \rangle$, $V(G(n,p)) = [n]$ such that the probability $\mathbb{P}\{(i,j) \in E(G(n,p))\} = p$ for any $(i,j) \in [n]^2$ (see Figure 3(a)). Then for any simple graph F, $t(F, G(n,p))$ is convergent with probability 1 to $p^{|E(F)|}$ as $n \to \infty$ [8]. Thus, $\{G(n,p)\}$ is a convergent sequence with the limit given by the constant graphon p. The pixel picture of $W_{G(n,p)}$ in Figure 3(b) provides the intuition behind the graph limit for $\{G(n,p)\}$. Note that for large n, the plot of the support of $W_{G(n,p)}$ resembles that of the constant function if looked at from a distance. In fact, the limiting graphon reflects the asymptotic density of connections in $G(n,p)$ as

Copyright © by SIAM. Unauthorized reproduction of this article is prohibited.

Downloaded 09/19/14 to 129.25.6.190. Redistribution subject to SIAM license or copyright; see http://www.siam.org/journals/ojsa.php

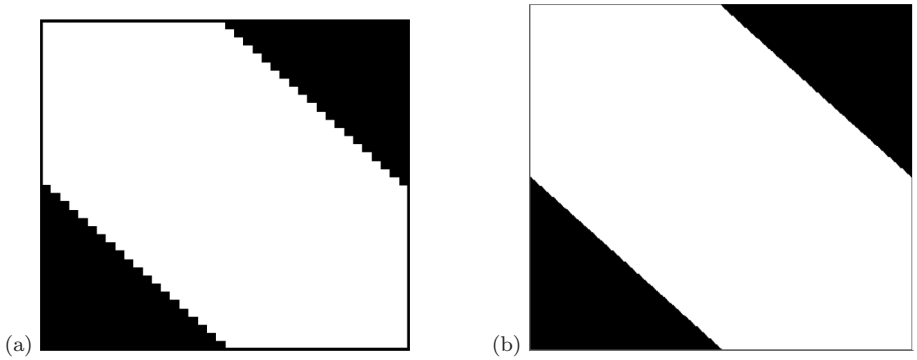

FIG. 4. (a) *The pixel picture of the half-graph* $H_{20,20}$. (b) *The limit of* $\{W_{H_{n,n}}\}$.

$n \to \infty$. Using the strong law of large numbers, one can show that $\|W_{G(n,p)} - p\|_\square \to 0$ as $n \to \infty$ with probability 1. Thus, $\{W_{G(n,p)}\}$ is convergent in the cut-norm but not in the L^1-norm.

Example 2.4 (see [26] the half-graphs). Let $H_{n,n} = \langle V(H_{n,n}), E(H_{n,n})\rangle$ be a bipartite graph on $2n$ nodes such that

$$V(H_{n,n}) = \{1, 2, \ldots, n, 1', 2', \ldots, n'\},\ E(H_{n,n}) = \{(i, j') \in V(H_{n,n}) \times V(H_{n,n}) :\ i \le j\}$$

(see Figure 4(a)). The sequence $\{H_{n,n}\}$ converges to the graphon H, where $H : I^2 \to I$ is the characteristic function of the set $\{(x, y) :\ |x - y| \ge 1/2\} \bigcap I^2$ (see Figure 4(b)). In this example, $\{W_{H_{n,n}}\}$ converges to H pointwise, and, by the dominated convergence theorem, in the L^1-norm.

3. The formulation of the problem.

3.1. The heat equation on discrete and continuous domains. Let $G_n = \langle V(G_n), E(G_n), W(G_n)\rangle$ be a sequence of weighted graphs, where $V(G_n) = [n]$ and $E(G_n)$ are the sets of nodes and edges, respectively; and $W(G_n) :\ [n]^2 \to [-1, 1]$ is a symmetric weight matrix of the form[3]

$$(W(G_n))_{ij} = \begin{cases} w_{ij}^{(n)}, & (i, j) \in E(G_n), \\ 0 & \text{otherwise.} \end{cases}$$

If G_n is a simple graph, $W(G_n)$ is a $\{0, 1\}$-valued matrix.

By the nonlinear heat equation on G_n we mean the system of differential equations

$$\frac{d}{dt} u_i^{(n)}(t) = n^{-1} \sum_{j=1}^{n} w_{ij}^{(n)} D\left(u_j^{(n)} - u_i^{(n)}\right),\ i \in [n], \tag{3.1}$$

where $u^{(n)}(t) = (u_1^{(n)}(t), u_2^{(n)}(t), \ldots, u_n^{(n)}(t))^{\mathsf{T}}$. The function $D :\ \mathbb{R} \to \mathbb{R}$ is Lipschitz continuous

$$|D(u) - D(v)| \le L|u - v|\ \forall u, v \in \mathbb{R}. \tag{3.2}$$

[3]For weighted graphs, one can also define convergence by extending the notion of the homomorphism density for this case (see [26] for details). We do not discuss this generalization here, because for the problems that we study in this paper a simpler (and stronger) form of convergence, convergence in L^1-norm, is sufficient (see section 5).

Copyright © by SIAM. Unauthorized reproduction of this article is prohibited.

Downloaded 09/19/14 to 129.25.6.190. Redistribution subject to SIAM license or copyright; see http://www.siam.org/journals/ojsa.php

Remark 3.1. Our analysis applies to a more general class of equations

$$\frac{d}{dt}u_i^{(n)}(t) = n^{-1}\sum_{j=1}^{n} w_{ij}^{(n)} D\left(u_j^{(n)} - u_i^{(n)}\right) + f_i(t, u_i^{(n)}),\ i \in [n], \tag{3.3}$$

where functions $f_i(t,u), i \in [n]$, can be taken, for instance, to be continuous in t and Lipschitz continuous in u:

$$|f_i(t,u) - f_i(t,v)| \le L|u-v|\ \forall u, v, t \in \mathbb{R},\ i \in [n].$$

To keep the presentation simple, we will restrict the analysis to the case of (3.1). It is straightforward to extend our results to cover (3.3).

If $D(u) = u$, the coupling operator on the right-hand side of (3.1) is the graph Laplacian, and (3.1) becomes the linear heat equation on G_n. The linear heat equation has many applications in combinatorial problems such as random walks on graphs [11], and dynamical problems, e.g., analysis of consensus protocols [28]. In this paper, we focus on the nonlinear heat equation, which provides the framework for a large class of dynamical networks. In particular, the Kuramoto equation (1.1) is of this type.

In the remainder of this paper, we will derive and justify the continuum counterpart of (3.1)

$$\frac{\partial}{\partial t}u(x,t) = \int_I W(x,y) D\left(u(y,t) - u(x,t)\right) dy. \tag{3.4}$$

The kernel W will be specified separately for each class of problems that we consider below.

3.2. The well-posedness of the IVP. Before setting out to study the relation between solutions of the discrete and continuous heat equations (3.1) and (3.4), we first address the well-posedness of the IVP for (3.4).

It is convenient to interpret the solution of the IVP for (3.4), $u(x,t)$, as a vector-valued map $\mathbf{u} : [0,T] \to L^\infty(I)$. Throughout this paper, we will use the bold font to denote the vector-valued function $\mathbf{u}(t)$ corresponding to a function of two variables $u(x,t)$.

THEOREM 3.2. *Suppose D is Lipschitz continuous, $W \in L^\infty(I^2)$, and $\mathbf{g} \in L^\infty(I)$. Then there exists a unique solution of the IVP for* (3.4) $\mathbf{u} \in C^1(\mathbb{R}; L^\infty(I))$ *subject to the initial condition* $\mathbf{u}(0) = \mathbf{g}$.

Proof. The proof of Theorem 3.2 is based on the contraction mapping principle (cf. [12, Theorem 1.1, Chapter VII]). We include the details for completeness.

Rewrite the IVP for (3.4) as the integral equation

$$\mathbf{u} = K\mathbf{u}, \tag{3.5}$$

where

$$[K\mathbf{u}](x,t) := \mathbf{g} + \int_0^t \int_I W(x,y) D\left(u(y,s) - u(x,s)\right) dyds.$$

Let $M_{\mathbf{g}}$ be a metric subspace of $C(0,\tau; L^\infty(I))$ (where $\tau > 0$ will be specified later) consisting of functions $\mathbf{u}$ satisfying $\mathbf{u}(0) = \mathbf{g}$. Then (3.5) is the fixed point equation for the operator $K : M_{\mathbf{g}} \to M_{\mathbf{g}}$. We show below that K is a contraction for a small $\tau > 0$.

Copyright © by SIAM. Unauthorized reproduction of this article is prohibited.

Downloaded 09/19/14 to 129.25.6.190. Redistribution subject to SIAM license or copyright; see http://www.siam.org/journals/ojsa.php

Downloaded 09/19/14 to 129.25.6.190. Redistribution subject to SIAM license or copyright; see http://www.siam.org/journals/ojsa.php

Indeed, let

$$\tau \le (4L\|W\|_{L^\infty(I^2)})^{-1}, \tag{3.6}$$

where L is the Lipschitz constant of $D(\cdot)$. For any $\mathbf{u}, \mathbf{v} \in M_{\mathbf{g}}$ we have

$$\begin{aligned}
&\|K\mathbf{u} - K\mathbf{v}\|_{M_{\mathbf{g}}} \\
&\quad = \max_{t\in[0,\tau]} \|K\mathbf{u}(t) - K\mathbf{v}(t)\|_{L^\infty(I)} \\
&\quad \le \max_{t\in[0,\tau]} \operatorname*{ess\,sup}_{x\in I} \int_{I\times[0,t]} |W(x,y)|\,|D\left(u(y,t)-u(x,t)\right) - D\left(v(y,t)-v(x,t)\right)|\,dydt \\
&\quad \le \tau L\|W\|_{L^\infty(I^2)} \max_{t\in[0,\tau]} \left\{ \int_I |u(y,t)-v(y,t)|\,dy + \|\mathbf{u}(t)-\mathbf{v}(t)\|_{L^\infty(I)} \right\} \\
&\quad \le 2\tau L\|W\|_{L^\infty(I^2)} \max_{t\in[0,\tau]} \|\mathbf{u}(t)-\mathbf{v}(t)\|_{L^\infty(I)}\,.
\end{aligned}$$

Thus, by (3.6) we have

$$\|K\mathbf{u} - K\mathbf{v}\|_{M_{\mathbf{g}}} \le \frac{1}{2}\|\mathbf{u}-\mathbf{v}\|_{M_{\mathbf{g}}}. \tag{3.7}$$

By the Banach contraction mapping principle, there exists a unique solution of the IVP for (3.4) $\bar{\mathbf{u}} \in M_{\mathbf{g}} \subset C(0,\tau;L^\infty(I))$. Using $\bar{\mathbf{u}}(\tau)$ as the initial condition, the local solution can be extended to $[0,2\tau]$, and, by repeating this argument, to $[0,T]$ for any $T>0$. In a similar fashion, we can prove the existence and uniqueness of the solution of the IVP for (3.4) on $[-T,0]$ for any $T>0$. Furthermore, since the integrand in (3.5) is continuous as a map $L^\infty(I)\to L^\infty(I)$, $\mathbf{u}$ is continuously differentiable. Thus, we have a classical solution of the IVP for (3.4) on the whole real axis. ∎

3.3. Spatial regularity. The classical heat equation, as a parabolic partial differential equation, has a strong smoothening property. Regardless of the regularity of the initial data, the solution of the IVP for the classical heat equation is a smooth function of the space variables for all positive times. No such mechanism is present in the heat equation on graph limits. Below we show that the spatial regularity of solutions of the IVP is determined by the regularity of graphon W and initial condition $\mathbf{u}(0)$.

THEOREM 3.3. *Let $D:\mathbb{R}\to\mathbb{R}$ be a Lipschitz continuous function and $J=(\alpha,\beta)\subset I$. Suppose for all $x\in J$ and for almost all $y\in I$, $W\in L^\infty(I^2)$ has a weak derivative $\frac{\partial}{\partial x}W(x,y)$ and*

$$\operatorname*{ess\,sup}_{y\in I} \left\| \frac{\partial}{\partial x} W(\cdot,y) \right\|_{L^2(J)} \le C_1 \tag{3.8}$$

for some $C_1>0$. Then for any $0<T<\infty$, all $t\in[0,T]$, and $\alpha<\alpha'<\beta'<\beta$, the solution of the IVP for (3.4) *satisfies*[4]

$$\mathbf{u}(t)\in H^1(J'),\ J'=(\alpha',\beta'),$$

provided $\mathbf{u}(0)\in L^\infty(I)\cap H^1(J)$.

[4] $H^1(J)$ stands for the Sobolev space of all Lebesgue measurable functions f on an open interval $J\subset\mathbb{R}^1$ such that f and its distributional derivative f_x are in $L^2(J)$ [10].

Copyright © by SIAM. Unauthorized reproduction of this article is prohibited.

Downloaded 09/19/14 to 129.25.6.190. Redistribution subject to SIAM license or copyright; see http://www.siam.org/journals/ojsa.php

Proof. Let $T > 0$ be arbitrary but fixed, and

$$h_0 = \frac{1}{2}\min\{\alpha' - \alpha, \beta - \beta'\}.$$

Then for $0 < h < h_0$, the difference quotient

$$\xi(x,t) = \frac{u(x+h,t) - u(x,t)}{h}$$

is a well-defined function on $\Omega_T = J' \times [0,T]$. Further, for $(x,t) \in \Omega_T$, $\xi(x,t)$ satisfies the following equation:

$$\begin{aligned}\frac{\partial}{\partial t}\xi(x,t) &= \int_I W(x,y)h^{-1}\left\{D\left(u(y,t) - u(x+h,t)\right) - D\left(u(y,t) - u(x,t)\right)\right\}dy \\ &\quad + \int_I D_x^h W(x,y) D\left(u(y,t) - u(x+h,t)\right)dy, \end{aligned} \tag{3.9}$$

where

$$D_x^h W(x,y) = \frac{W(x+h,y) - W(x,y)}{h}.$$

By multiplying both sides of (3.9) by $\xi(x,t)$ and integrating both sides of the resultant equation over J' with respect to x, we have

$$\begin{aligned}&\frac{1}{2}\int_{J'} \frac{\partial}{\partial t}\xi(x,t)^2 dx \\ &\quad = \int_{J'\times I} W(x,y)h^{-1}\left\{D\left(u(y,t) - u(x+h,t)\right) - D\left(u(y,t) - u(x,t)\right)\right\}\xi(x,t)dxdy \\ &\qquad + \int_{J'\times I} D_x^h W(x,y) D\left(u(y,t) - u(x+h,t)\right)\xi(x,t)dxdy \\ &\quad =: T_1 + T_2. \end{aligned} \tag{3.10}$$

Using $\mathbf{u} \in C(0,T;L^\infty(I))$, Lipschitz continuity of $D(\cdot)$, and the triangle inequality, we have

$$\max_{t\in[0,T]} \operatorname*{ess\,sup}_{(x,y)\in I^2} |D(u(y,t) - u(x,t))| \le 2L\|\mathbf{u}\|_{C(0,T;L^\infty(I))} =: C_2. \tag{3.11}$$

Furthermore, using Fubini's theorem, (3.8), and the standard results for the difference quotients (see, e.g., Theorem 5.8.3 [14]), we have

$$\|D_x^h W\|_{L^2(J'\times I)} \le \operatorname*{ess\,sup}_{y\in I} \|D_x^h W\|_{L^2(J')} \le C_3 \operatorname*{ess\,sup}_{y\in I} \left\| \frac{\partial}{\partial x} W(\cdot, y)\right\|_{L^2(J)} \le C_4, \tag{3.12}$$

and, likewise,

$$\|\boldsymbol{\xi}(0)\|_{L^2(J')} \le C_5 \|\mathbf{u}(0)\|_{H^1(J)}, \tag{3.13}$$

where positive constants C_3, C_4, and C_5 are independent of $h \in (0, h_0)$. Recall that $\boldsymbol{\xi}(t)$ stands for the vector-valued function corresponding to $\xi(x,t)$.

Copyright © by SIAM. Unauthorized reproduction of this article is prohibited.

Downloaded 09/19/14 to 129.25.6.190. Redistribution subject to SIAM license or copyright; see http://www.siam.org/journals/ojsa.php

Using (3.2), we bound the first term on the right-hand side (3.10)

$$|T_1| \le \|W\|_{L^\infty(I^2)} \int_{J'\times I} L\xi(x,t)^2 dxdy = L\|W\|_{L^\infty(I^2)} \|\boldsymbol{\xi}(t)\|^2_{L^2(J')}. \tag{3.14}$$

For the second term, we use (3.11), (3.12), and the Cauchy–Schwarz inequality

$$\begin{aligned} |T_2| &\le C_2 \int_{J'\times I} \left|D_x^h W \boldsymbol{\xi}(t)\right| dxdy \le C_2 \|D_x^h W\|_{L^2(J'\times I)} \|\boldsymbol{\xi}(t)\|_{L^2(J')} \\ &\le C_2 C_4 \|\boldsymbol{\xi}(t)\|_{L^2(J')}. \end{aligned} \tag{3.15}$$

By combining (3.10), (3.14), and (3.15), we have

$$\frac{d}{dt}\|\boldsymbol{\xi}(t)\|^2_{L^2(J')} \le C_6 \|\boldsymbol{\xi}(t)\|^2_{L^2(J')} + C_7,\ C_6 = 2L\|W\|_{L^\infty(I^2)} + C_7,\ C_7 = C_2 C_4,$$

where inequality $2\|\boldsymbol{\xi}(t)\|_{L^2(J')} \le \|\boldsymbol{\xi}(t)\|^2_{L^2(J')} + 1$ was used. Using Gronwall's inequality, we obtain

$$\begin{aligned} \|\boldsymbol{\xi}(t)\|^2_{L^2(J')} &\le \left(\|\boldsymbol{\xi}(0)\|^2_{L^2(J')} + \frac{C_7}{C_6}\right) \exp\{C_6 T\} \\ &\le \left(C_5^2 \|\mathbf{u}(0)\|^2_{H^1(J)} + \frac{C_7}{C_6}\right) \exp\{C_6 T\},\ t \in [0,T]. \end{aligned} \tag{3.16}$$

The last inequality yields a uniform in $h \in (0, h_0]$ bound on the difference quotient $\|\boldsymbol{\xi}(t)\|_{L^2(J')}$. Using the properties of the difference quotients (cf. Theorem 5.8.3 [14]), we conclude that $\mathbf{u}(t) \in H^1(J')$ for all $t \in (0,T]$. ∎

4. Networks on simple graphs. In this and in the following sections, we prove that the solution of the IVP for appropriately chosen continuous problem (3.4) approximates the solutions of the discrete problems (3.1) when n is sufficiently large. We prove this result for two classes of convergent graph sequences. In this section, we consider the case of a sequence of simple graphs converging to a $\{0,1\}$-valued graphon, and we study a more general case of convergent sequences of weighted graphs in the next section. We single out networks on $\{0,1\}$-valued graphons for two reasons. First, many coupled oscillator models fit into this framework (see, e.g., [46, 17] and section 6.2). Second, for this class of networks we can explicitly estimate the accuracy of approximation of the solutions of the discrete models by those of their continuum limits in terms of the network size and the geometry of the graphon of the network (cf. Theorem 4.1). This result is important, because it reveals the structural properties of the graphs shaping the accuracy of the thermodynamic limit.

Let $W : I^2 \to \{0,1\}$ be a symmetric measurable function. We denote the support of W by

$$W^+ = \overline{\{(x,y) \in I^2 :\ W(x,y) \ne 0\}} \tag{4.1}$$

and its boundary by ∂W^+.

For convenience, we rewrite the IVP for (3.4)

$$\frac{\partial}{\partial t} u(x,t) = \int_I W(x,y) D\left(u(y,t) - u(x,t)\right) dy, \tag{4.2}$$

$$u(x,0) = g(x), \tag{4.3}$$

where $\mathbf{g} \in L^\infty(I)$.

Copyright © by SIAM. Unauthorized reproduction of this article is prohibited.

Downloaded 09/19/14 to 129.25.6.190. Redistribution subject to SIAM license or copyright; see http://www.siam.org/journals/ojsa.php

Next, we define a sequence of discrete problems. To this end, we fix $n \in \mathbb{N}$, divide I into n subintervals

$$I_1^{(n)} = \left[0, \frac{1}{n}\right),\ I_2^{(n)} = \left[\frac{1}{n}, \frac{2}{n}\right), \dots, I_n^{(n)} = \left[\frac{n-1}{n}, 1\right), \tag{4.4}$$

and define a sequence of simple graphs $G_n = \langle V(G_n), E(G_n)\rangle$ such that $V(G_n) = [n]$ and

$$E(G_n) = \{(i,j) \in [n]^2 :\ (I_i^{(n)} \times I_j^{(n)}) \cap W^+ \neq \emptyset\}.$$

The IVP for the nonlinear heat equation on $\{G_n\}$, a discrete counterpart of (4.2), is given by

$$\frac{d}{dt}u_i^{(n)}(t) = n^{-1} \sum_{j:(i,j)\in E(G_n)} D(u_j^{(n)} - u_i^{(n)}), \tag{4.5}$$

$$u_i^{(n)}(0) = g_i^{(n)},\ i \in [n], \tag{4.6}$$

where

$$g_i^{(n)} = n \int_{I_i^{(n)}} g(x)dx \tag{4.7}$$

is the average value of $g(x)$ on $I_i^{(n)}$. To compare the solutions of the discrete and continuous models, it is convenient to represent the discrete function $u^{(n)}(t) = (u_1^{(n)}(t), u_2^{(n)}(t), \dots, u_n^{(n)}(t))^{\mathsf{T}}$ as a step function on I as follows:

$$u_n(x,t) = u_i^{(n)}(t) \text{ if } x \in I_i^{(n)}. \tag{4.8}$$

Then $u_n(x,t)$ satisfies the following IVP:

$$\frac{\partial}{\partial t}u_n(x,t) = \int_I \hat{W}_n(x,y) D\left(u_n(y,t) - u_n(x,t)\right) dy, \tag{4.9}$$

$$u(x,0) = g_n(x), \tag{4.10}$$

where

$$g_n(x) = g_i^{(n)} \text{ if } x \in I_i^{(n)}, i \in [n],$$

and $\hat{W}_n(x,y)$ is the step function such that for $(x,y) \in I_i^{(n)} \times I_j^{(n)}$, $(i,j) \in [n]^2$,

$$\hat{W}_n(x,y) = \begin{cases} 1 & \text{if } (I_i^{(n)} \times I_j^{(n)}) \cap W^+ \neq \emptyset, \\ 0 & \text{otherwise.} \end{cases} \tag{4.11}$$

The rate of convergence of the solutions of discrete problems (4.9), (4.10) to those of the limiting problem (4.2), (4.3) depends on the regularity of ∂W^+ (cf. (4.1)). To this end, we recall the upper box-counting dimension of ∂W^+ as a subset of $\mathbb{R}^2$:

$$\overline{\dim}_B \partial W^+ = \overline{\lim_{\delta \to 0}} \frac{\log N_\delta(\partial W^+)}{-\log \delta}, \tag{4.12}$$

Copyright © by SIAM. Unauthorized reproduction of this article is prohibited.

where $N_\delta(\partial W^+)$ is the number of cells of a $(\delta \times \delta)$-mesh that intersect ∂W^+ (see equation (3.12)(iv) in [15]).

THEOREM 4.1. *Suppose* $\mathbf{g} \in L^\infty(I)$, $W : I^2 \to \{0,1\}$ *is a symmetric measurable function and*

$$\gamma := \overline{\dim}_B \partial W^+ \in [0,2). \tag{4.13}$$

Let $\mathbf{u}$ *and* $\mathbf{u}_n$ *denote the vector-valued functions corresponding to the solutions of* (4.2), (4.3), *and* (4.9)–(4.11), *respectively.*

Then for any $\epsilon > 0$ *there exists* $N(\epsilon) \in \mathbb{N}$ *such that for* $n \geq N(\epsilon)$

$$\|\mathbf{u} - \mathbf{u}_n\|_{C(0,T;L^2(I))} \leq C_1 \left(\|\mathbf{g} - \mathbf{g}_n\|_{L^2(I)} + n^{-(1-\gamma/2-\epsilon)} \right), \tag{4.14}$$

where constant C_1 *is independent of* n.[5]

Remark 4.2. In particular, if $\mathbf{g}$ is a step function, so that $\|\mathbf{g} - \mathbf{g}_n\|^2_{L^2(I)} = O(n^{-1})$, and $\gamma \geq 1$, the rate of convergence in (4.14) is determined by the fractal dimension of the boundary ∂W^+.

Remark 4.3. The box-counting dimension of the boundary of support of W comes up naturally in the proof of Theorem 4.1, as it determines the L^2-accuracy of approximation of the $\{0,1\}$-valued graphon W by the step functions $\hat{W}_n$.

Proof. Denote $\xi_n(x,t) = u_n(x,t) - u(x,t)$. By subtracting (4.2) from (4.9), we have

$$\begin{aligned} \frac{\partial \xi_n}{\partial t} &= \int_I \hat{W}_n(x,y) \left\{ D\left(u_n(y,t) - u_n(x,t)\right) - D\left(u(y,t) - u(x,t)\right) \right\} dy \\ &\quad + \int_I \left(\hat{W}_n(x,y) - W(x,y) \right) D\left(u(y,t) - u(x,t)\right) dy. \end{aligned} \tag{4.15}$$

Next, we multiply both sides of (4.15) by $\xi_n(x,t)$ and integrate over I

$$\begin{aligned} &\frac{1}{2} \int_I \frac{\partial}{\partial t} \xi_n(x,t)^2 dx \\ &\quad = \int_{I^2} \hat{W}_n(x,y) \left\{ D\left(u_n(y,t) - u_n(x,t)\right) - D\left(u(y,t) - u(x,t)\right) \right\} \xi_n(x,t) dx dy \\ &\quad + \int_{I^2} \left(\hat{W}_n(x,y) - W(x,y) \right) D\left(u(y,t) - u(x,t)\right) \xi_n(x,t) dx dy. \end{aligned} \tag{4.16}$$

Using the Lipschitz continuity of $D(\cdot)$, $\|\hat{W}\|_{L^\infty(I^2)} = 1$, the triangle inequality, and the Cauchy–Schwarz inequality, we estimate the first term on the right-hand side of (4.16)

$$\begin{aligned} &\left| \int_{I^2} \hat{W}_n(x,y) \left\{ D\left(u_n(y,t) - u_n(x,t)\right) - D\left(u(y,t) - u(x,t)\right) \right\} \xi_n(x,t) dx dy \right| \\ &\qquad \leq L \int_{I \times I} \left| \left(\xi_n(y,t) - \xi_n(x,t)\right) \xi_n(x,t) \right| dx dy \leq 2L \|\boldsymbol{\xi}_n(t)\|^2_{L^2(I^2)}. \end{aligned} \tag{4.17}$$

[5] $\|\cdot\|_{C(0,T;L^2(I))}$ stands for the norm in the space of continuous vector-valued function $\mathbf{u} : [0,T] \to L^2(I)$ [14].

Copyright © by SIAM. Unauthorized reproduction of this article is prohibited.

Downloaded 09/19/14 to 129.25.6.190. Redistribution subject to SIAM license or copyright; see http://www.siam.org/journals/ojsa.php

Downloaded 09/19/14 to 129.25.6.190. Redistribution subject to SIAM license or copyright; see http://www.siam.org/journals/ojsa.php

We estimate the second term on the right-hand side of (4.16), using the Cauchy–Schwarz inequality and the bound on $D(\cdot)$ (cf. (3.11))

$$\begin{aligned}&\left|\int_{I^2}\left(\hat W_n(x,y)-W(x,y)\right)D\left(u(y,t)-u(x,t)\right)\xi_n(x,t)dxdy\right|\\&\quad\le \operatorname*{ess\,sup}_{(x,y,t)\in I^2\times[0,T]}\left|D\left(u(y,t)-u(x,t)\right)\right|,\\&\qquad\left|\int_{I^2}\left(\hat W_n(x,y)-W(x,y)\right)\xi_n(x,t)dxdy\right|\\&\quad\le C_2\|W-\hat W_n\|_{L^2(I^2)}\|\boldsymbol{\xi}_n\|_{L^2(I)}\end{aligned}\tag{4.18}$$

for some constant $C_2>0$ independent of n.

Using (4.17) and (4.18), from (4.16) we have

$$\frac{d}{dt}\|\boldsymbol{\xi}_n\|^2_{L^2(I)}\le 4L\|\boldsymbol{\xi}_n\|^2_{L^2(I)}+2C_2\|W-\hat W_n\|_{L^2(I^2)}\|\boldsymbol{\xi}_n\|_{L^2(I)}.\tag{4.19}$$

Let $\varepsilon>0$ be arbitrary but fixed, and set

$$\phi_\varepsilon(t)=\sqrt{\|\boldsymbol{\xi}_n\|^2_{L^2(I)}+\varepsilon}.$$

By (4.19),

$$\frac{d}{dt}\phi_\varepsilon(t)^2\le 4L\phi_\varepsilon(t)^2+2C_2\|W-\hat W_n\|_{L^2(I^2)}\phi_\varepsilon(t).\tag{4.20}$$

Since $\phi_\varepsilon(t)$ is positive on $[0,T]$, from (4.20), we have

$$\frac{d}{dt}\phi_\varepsilon(t)\le 2L\phi_\varepsilon(t)+C_2\|W-\hat W_n\|_{L^2(I^2)},\ t\in[0,T].$$

By Gronwall's inequality,

$$\sup_{t\in[0,T]}\phi_\varepsilon(t)\le\left(\phi_\varepsilon(0)+\frac{C_2\|W-\hat W_n\|_{L^2(I^2)}}{2L}\right)\exp\{2LT\}.\tag{4.21}$$

Since $\varepsilon>0$ is arbirtrary, (4.21) implies

$$\sup_{t\in[0,T]}\|\boldsymbol{\xi}_n(t)\|_{L^2(I)}\le\left(\|\mathbf{g}-\mathbf{g}_n\|_{L^2(I)}+\frac{C_2\|W-\hat W_n\|_{L^2(I^2)}}{2L}\right)\exp\{2LT\}.\tag{4.22}$$

It remains to estimate $\|W-\hat W_n\|_{L^2(I^2)}$. To this end, consider the set of discrete cells $I_i^{(n)}\times I_j^{(n)}$ that covers the boundary of the support of W

$$J(n)=\{(i,j)\in[n]^2:\ (I_i^{(n)}\times I_j^{(n)})\cap\partial W^+\ne\emptyset\}\text{ and }C(n)=|J(n)|.$$

Using (4.12) and (4.13), for any $\epsilon>0$ and sufficiently large n, we have

$$C(n)\le n^{\gamma+2\epsilon}.$$

Since W and $\hat W_n$ coincide almost everywhere on cells $I_i^{(n)}\times I_j^{(n)}$, for which $(i,j)\notin J(n)$, for any $\epsilon>0$ and all sufficiently large n, we have

$$\|W-\hat W_n\|^2_{L^2(I^2)}=\int_{I^2}(W-\hat W_n)^2dxdy\le C(n)n^{-2}\le n^{-2(1-\gamma/2-\epsilon)}.\tag{4.23}$$

The combination of (4.22) and (4.23) yields (4.14). ∎

Copyright © by SIAM. Unauthorized reproduction of this article is prohibited.

Downloaded 09/19/14 to 129.25.6.190. Redistribution subject to SIAM license or copyright; see http://www.siam.org/journals/ojsa.php

5. Networks on weighted graphs. In this section, we study a more general case of the heat equation on convergent sequences of weighted graphs. First, we define two graph sequences generated by a given graphon W and then we prove the convergence of the corresponding discrete problems to the continuum limit (4.2).

Throughout this section, we assume that $W : I^2 \to [-1, 1]$ is a symmetric measurable function. Function W will be used to assign weights to the edges of the graphs considered below. We allow for both positive and negative weights. Let $\mathcal{P}_n$ denote the partition of I into n intervals, $\mathcal{P}_n = \{I_i^{(n)}, i \in [n]\}$ (see (4.4)) and

$$X_n = \left\{ \frac{1}{n}, \frac{2}{n}, \dots, \frac{n}{n} \right\}.$$

The quotient of W and $\mathcal{P}_n$, denoted $W/\mathcal{P}_n$, is a weighted graph on n nodes

$$W/\mathcal{P}_n = \langle [n], [n] \times [n], \bar{W}_n \rangle,$$

such that weights $(\bar{W}_n)_{ij}$ are obtained by averaging W over the sets in $\mathcal{P}_n$

$$(\bar{W}_n)_{ij} = n^2 \int_{I_i^{(n)} \times I_j^{(n)}} W(x, y) dx dy. \tag{5.1}$$

The second sequence of weighted graphs is obtained in a way that is similar to the construction of W-random graph (cf. [26])

$$\mathbb{H}(X_n, W) = \langle [n], [n] \times [n], \tilde{W}_n \rangle, \ (\tilde{W}_n)_{ij} = W\left(\frac{i}{n}, \frac{j}{n} \right). \tag{5.2}$$

In the remainder of this section, we prove convergence of the nonlinear heat equations on $W/\mathcal{P}_n$ and $\mathbb{H}(X_n, W)$ to the continuum equation on the graphon W (cf. (4.2)). Furthermore, we show that the former problems correspond to the discretizations of (4.2) using the method of Galerkin and the collocation method, respectively, thus, relating the problem of justification of the thermodynamic limit for dynamical networks to two well-known numerical schemes for equations of mathematical physics.

We first consider the IVP for the heat equation on $W/\mathcal{P}_n$

$$\frac{d}{dt} u_i^{(n)}(t) = n^{-1} \sum_{j=1}^{n} (\bar{W}_n)_{ij} D\left(u_j^{(n)}(t) - u_i^{(n)}(t) \right), \tag{5.3}$$

$$u_i^{(n)}(0) = g_i^{(n)}, \ i \in [n], \tag{5.4}$$

where $g_i^{(n)}$ is defined in (4.7).

By associating the step function $u_n(x, t)$ with $u^{(n)}(t)$ (see (4.8)), we rewrite (5.3) and (5.4) as

$$\frac{\partial}{\partial t} u_n(x, t) = \int_I W_n(x, y) D\left(u_n(y, t) - u_n(x, t) \right) dy, \tag{5.5}$$

$$u_n(x, 0) = g_n(x), \tag{5.6}$$

where W_n and g_n are the step functions

$$W_n(x, y) = (\bar{W}_n)_{ij} \text{ for } (x, y) \in I_i^{(n)} \times I_j^{(n)},$$
$$g_n(x) = g_i^{(n)} \text{ for } x \in I_i^{(n)}, \ i \in [n].$$

Copyright © by SIAM. Unauthorized reproduction of this article is prohibited.

Downloaded 09/19/14 to 129.25.6.190. Redistribution subject to SIAM license or copyright; see http://www.siam.org/journals/ojsa.php

Remark 5.1. It is instructive to note that (5.3) and (5.4) can be viewed as the Galerkin approximation of the IVP (4.2) and (4.3). Indeed, let H_n denote a finite-dimensional subspace of $L^2(I)$

$$H_n = \operatorname{span}\{\phi_1^{(n)}, \phi_2^{(n)}, \dots, \phi_n^{(n)}\},\ i \in [n],$$

where $\phi_i^{(n)} = \chi_{I_i^{(n)}}$ is the characteristic function of $I_i^{(n)} = [(i-1)n^{-1}, in^{-1})$.

Replacing $u(x,t)$ in (4.2) with

$$u_n(x,t) = \sum_{k=1}^{n} u_k^{(n)}(t)\phi_k^{(n)}(x) \in H_n$$

and projecting the resultant equation on H_n, we arrive at (5.3).

THEOREM 5.2. *Suppose $W : I^2 \to [-1,1]$ is a symmetric measurable function and $\mathbf{g} \in L^\infty(I)$. Let $\mathbf{u}$ and $\mathbf{u}_n$ be the solutions of* (4.2), (4.3) *and* (5.5), (5.6), *respectively. Then*

$$\|\mathbf{u} - \mathbf{u}_n\|_{C(0,T;L^2(I))} \to 0 \text{ as } n \to \infty. \tag{5.7}$$

Proof. By following the lines of the proof of Theorem 4.1 (see (4.22)), for $\xi_n(x,t) = u_n(x,t) - u(x,t)$, we obtain

$$\sup_{t\in[0,T]} \|\boldsymbol{\xi}_n(t)\|_{L^2(I)} \le \left(\|\mathbf{g} - \mathbf{g}_n\|_{L^2(I)}^2 + \frac{C_1\|W - W_n\|_{L^2(I^2)}}{C_2}\right)\exp\{C_2 T\}, \tag{5.8}$$

where positive constants C_1 and C_2 are independent of n. By the Lebesgue differentiation theorem,

$$W_n \to W \text{ and } \mathbf{g}_n \to \mathbf{g},\ \text{as } n \to \infty,$$

almost everywhere on I^2 and I, respectively. Thus, the statement of the theorem follows from (5.8) via the dominated convergence theorem. ∎

The heat equation on $\mathbb{H}(X_n, W)$ is analyzed in complete analogy to the IVP for $W/\mathcal{P}_n$. The IVP in this case remains (5.5) and (5.6) modulo the definition of the step function

$$W_n(x,y) = W\left(\frac{i}{n}, \frac{j}{n}\right) \text{ for } (x,y) \in I_i^{(n)} \times I_j^{(n)},\ (i,j) \in [n]^2. \tag{5.9}$$

We assume that $W(x,y)$ is a bounded symmetric measurable function that is almost everywhere continuous on I^2. By construction of W_n (cf. (5.9)),

$$W_n(x,y) \to W(x,y),\ \text{as } n \to \infty$$

at every point of continuity of W, i.e., almost everywhere. Thus, by the dominated convergence theorem, we have

$$\|W - W_n\|_{L^2(I^2)} \to 0 \text{ as } n \to \infty.$$

With this observation, the proof of Theorem 5.2 applies to the situation at hand. Thus, we have the following theorem.

THEOREM 5.3. *Suppose $W : I^2 \to [-1,1]$ is a symmetric measurable function, which is continuous almost everywhere on I^2, and $\mathbf{g} \in L^\infty(I)$. Let $\mathbf{u}$ and $\mathbf{u}_n$ be the solutions of* (4.2), (4.3) *and* (5.5), (5.6), (5.9), *respectively. Then*

$$\|\mathbf{u} - \mathbf{u}_n\|_{C(0,T;L^2(I))} \to 0 \text{ as } n \to \infty. \tag{5.10}$$

Copyright © by SIAM. Unauthorized reproduction of this article is prohibited.

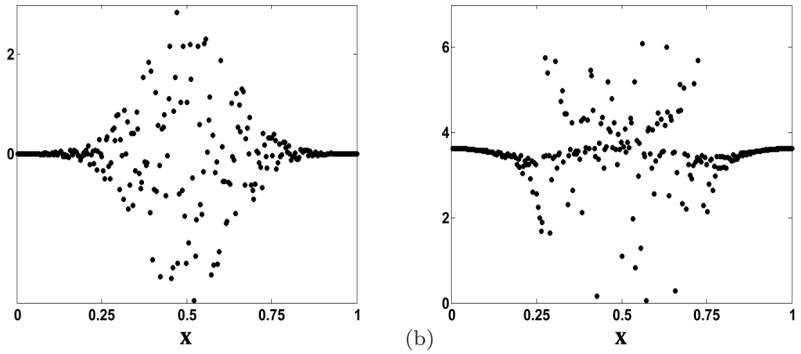

FIG. 5. (a) *The initial conditions* (6.2) *for the chimera state shown in* (b). (b) *A snapshot of the solution of* (6.1) *and* (6.2), $\phi(x,t)$ *for a fixed* $t > 0$.

6. Examples. In this section, we illustrate the results of this paper with several examples. First, we apply Theorem 3.3 to explain the regions of continuity in the chimera states [19]. Next, we discuss the attractors of the system of Kuramoto oscillators on multipartite graphs.

6.1. Regions of continuity of chimera states. Chimera states are persistent patterns of coexisting regions of spatially coherent and chaotic behaviors (see Figure 5(b)). They were discovered by Kuramoto and Battogtokh in the following continuum limit of a system of coupled phase oscillators [19]:

$$\frac{\partial}{\partial t}\phi(x,t) = \omega + \int_0^1 G(x-y)\sin\left(\phi(y,t) - \phi(x,t) + \alpha\right) dy. \tag{6.1}$$

Function $\phi:\ I \times \mathbb{R}^+ \to \mathbb{S}^1 := \mathbb{R}/2\pi\mathbb{Z}$ describes the evolution of the phase of oscillator at $x \in I$. The exponential kernel $G(x) = \exp\{-\kappa|x|\}$ provides nonlocal coupling between oscillators. Equation (6.1) was obtained using the phase reduction from the Ginzburg–Landau equation, which describes collective dynamics of nonlocally coupled limit cycle oscillators (cf. [19]). The sequences of discrete problems converging to (6.1) can be obtained using one of the schemes of section 5.

The Kuramoto–Battogtokh model was the first example of a coupled system of identical oscillators featuring robust patterns that combine coherent and irregular dynamics. Since then, chimera states were demonstrated in a variety of computational and experimental settings [22, 42, 23]. The precise mathematical mechanism underlying these patterns is the subject of ongoing research [33]. Here, we focus on one aspect of the chimera states: the regions of continuity. Specifically, we use Theorem 3.3 to explain why the synchronous dynamics is restricted to the two subdomains of I (see Figure 5(a)). We show that this is possible because of the lack of the smoothening property of the heat equation on graph limits, which is one important distinction from the classical heat equation.

The numerical generation of the chimera states in (6.1) requires a careful setup, which we review next. To trigger a chimera state one has to start with the appropriate initial conditions; otherwise oscillators end up evolving in phase. Abrams and Strogatz reported that they were unable to generate chimera states in (6.1) from smooth initial conditions [1]. Instead, one has to initialize the system with the initial condition that combines the regions of coherent and incoherent spatial profiles. The following initial condition for the numerical generation of chimera states was suggested by

Copyright © by SIAM. Unauthorized reproduction of this article is prohibited.

Downloaded 09/19/14 to 129.25.6.190. Redistribution subject to SIAM license or copyright; see http://www.siam.org/journals/ojsa.php

Downloaded 09/19/14 to 129.25.6.190. Redistribution subject to SIAM license or copyright; see http://www.siam.org/journals/ojsa.php

Kuramoto (cf. [1]):

(6.2)
$$\phi(x_i,0)=h(x_i)r_i,\ \text{where } h(x)=6\exp\left\{-30\left(x_i-(1/2)\right)^2\right\},\ x_i=in^{-1},\ i\in[n],$$

and r_i are independent random variables drawn from the uniform distribution on $(-1/2,1/2)$ (see Figure 5(a)). The values of the other parameters are $\kappa=4$, $\alpha=1.457$ (cf. [1]). Numerical integration of (6.1) and (6.2) with these parameter values yields persistent patterns with coexisting regions of spatially coherent and chaotic dynamics. A representative snapshot is shown in Figure 5(b).

Theorem 3.3 explains the role of the initial conditions in generating chimera states. Note that function $h(x)$ in (6.2) rapidly decays to 0 outside a neighborhood of $1/2$. Therefore, the initial conditions in the intervals $J_1=(0,0.2)$ and $J_2=(0.8,1)$ near the endpoints of the interval $[0,1]$ for all practical purposes can be viewed as if they were produced by discretization of a function that is smooth over J_1 and J_2 (see Figure 5(a)). For such initial conditions, Theorem 3.3 implies that the solution $\phi(x,t)$ will remain continuous on J_1 and J_2, because $H^1(J_{1,2})\subset C(J_{1,2})$ by the Sobolev embedding theorem [14]. This explains why the spatial profile remains coherent over J_1 and J_2 for positive times (see Figure 5(b)). Theorem 3.3 also implies that it is impossible to generate chimera states starting from smooth initial data, because for such data the solution of the continuum limit remains continuous over the entire domain for all $t>0$. This rules out regions of chaotic behavior in large networks, because their solutions remain close to that of the continuous system by Theorem 5.2 or Theorem 5.3. This explains failed attempts to produce chimera states from smooth initial conditions in [1].

6.2. The Kuramoto equation on multipartite graphs. To illustrate our results for networks on simple graphs (cf. section 4), we discuss the Kuramoto equation on multipartite graphs. The examples of this subsection illustrate another implication of the lack of smoothening property of the heat equation on graph limits. This time we show that the lack of smoothness of the limiting graphon may result in stable discontinuous patterns.

Consider the Kuramoto equation on the sequence of bipartite complete graphs

$$\dot{u}_i^{(n)}(t)=\frac{(-1)^\sigma}{n}\sum_{j:\ (j,i)\in E(K_{n,n})}\sin\left(u_j^{(n)}(t)-u_i^{(n)}(t)\right),\quad i\in[2n], \tag{6.3}$$

where

$$K_{n,n}=\langle[2n],E(K_{n,n})\rangle\ \text{ and }\ E(K_{n,n})=\{(i,j)\in[n]^2:\ 1\le i\le n<j\le 2n\}.$$

The sequence $\{K_{n,n}\}$ is convergent with the limit shown in Figure 6(a). We consider two models for $\sigma=0$ and $\sigma=1$. As shown below, the space homogeneous (synchronous) solution is stable for the $\sigma=0$ model and is unstable if $\sigma=1$ (see Figure 6(b), (c)).

Along with (6.3) we consider its continuum limit

$$\frac{\partial}{\partial t}u(x,t)=(-1)^\sigma\int_I K(x,y)\sin\left(u(y,t)-u(x,t)\right)dy, \tag{6.4}$$

where graphon $K\in\mathcal{W}_0$ is the limit of $\{K_{n,n}\}$ (see Figure 6(a)). Fix $y\in I$ and consider $K(x,y)$ as a function of x. Because $K(x,y)$ has a jump discontinuity at $x=1/2$, it

Copyright © by SIAM. Unauthorized reproduction of this article is prohibited.

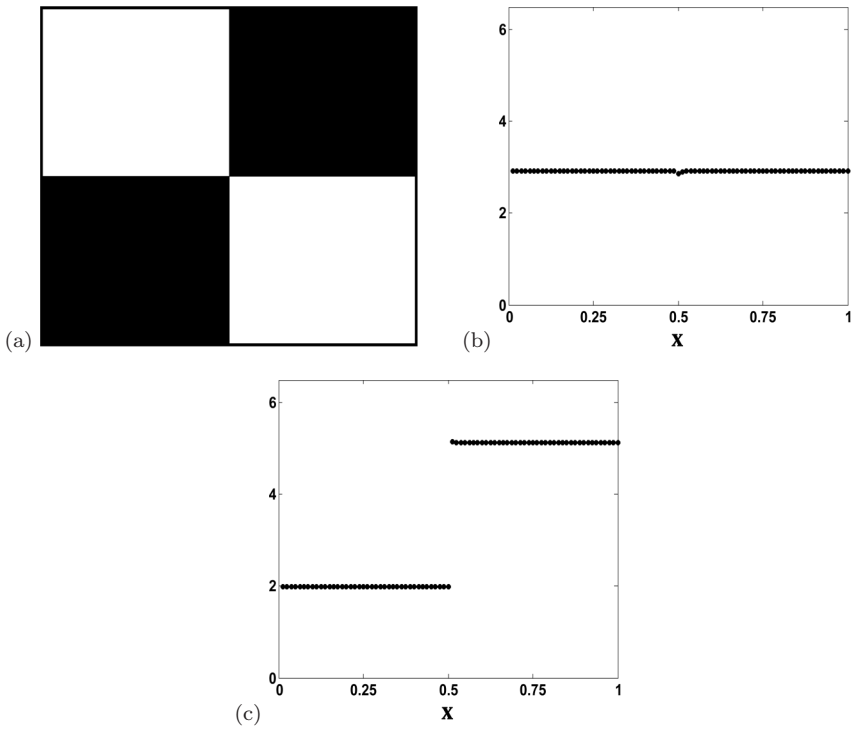

FIG. 6. (a) *The plot of support of* $W_{K_{n,n}}$. (b), (c) *Solutions of the IVP problem for the Kuramoto equation on the bipartite complete graphs converge to the synchronous solution for* $\sigma = 0$ (b) *and to the step function for* $\sigma = 1$ (c).

does not have a weak derivative $\frac{\partial}{\partial x}K(x,y)$ on any interval in x that contains $1/2$. However, we can apply Theorem 3.3 on any open interval $J \subset (0,1/2) \cup (1/2,1)$ to conclude that $u(x,t)$ restricted to any interval $J' \subset J$ is in $H^1(J')$ for any $t > 0$, provided $u(\cdot,0) \in L^\infty(I) \cap H^1(J)$. By the Sobolev embedding theorem [14], $u(x,t) \in \tilde{C}(I)$ for any $t > 0$, where

$$\tilde{C}(I) = \{u \in L^\infty(I) : \text{ for any open interval } J \subset (0,1/2) \cup (1/2,1)\ u\,|_J \in C(J)\}.$$

Here, by $u\,|_J$ we denote the restriction of u to J.

Since solutions of the IVPs for (6.4) with appropriate initial data belong to $\tilde{C}(I)$, we restrict our search for attractors of (6.4) to functions from this class. Thus, we look for steady state solutions of (6.4) that belong to $\tilde{C}(I)$. For simplicity, we focus on piecewise constant solutions from this class. Setting the right-hand side of (6.4) to 0, we obtain

$$\int_{1/2}^{1} \sin\left(u(y,t) - u(x,t)\right) dy = 0, x \in (0,1/2), \tag{6.5}$$

$$\int_{0}^{1/2} \sin\left(u(y,t) - u(x,t)\right) dy = 0, x \in (1/2,1). \tag{6.6}$$

From (6.5) and (6.6), we find that the only piecewise constant steady state solutions from $\tilde{C}(I)$ are the space homogeneous function

$$u^h(x) = c \text{ for } x \in [0,1]$$

Copyright © by SIAM. Unauthorized reproduction of this article is prohibited.

Downloaded 09/19/14 to 129.25.6.190. Redistribution subject to SIAM license or copyright; see http://www.siam.org/journals/ojsa.php

Downloaded 09/19/14 to 129.25.6.190. Redistribution subject to SIAM license or copyright; see http://www.siam.org/journals/ojsa.php

and the step function

$$u^s(x) = \begin{cases} c_1, & x \in [0, 1/2), \\ c_2, & x \in [1/2, 1], \end{cases}$$

where constants $c, c_1, c_2 \in \mathbb{S}^1$ and $|c_2 - c_1| = \pi$.

Next, we turn to the discrete model (6.3). The discrete counterparts of $u^s(x,t)$ and $u^h(x,t)$ are

$$u^h = c\mathbf{1}_{2n} \in \mathbb{R}^{2n} \text{ and } u^s = (c_1\mathbf{1}_n^\mathsf{T}, c_2\mathbf{1}_n^\mathsf{T}) \in \mathbb{R}^{2n},$$

where $\mathbf{1}_n = (1, 1, \dots, 1)^\mathsf{T} \in \mathbb{R}^n$.

The linearization of (6.3) about $u = u^h$ yields

$$\dot{\xi} = \frac{(-1)^{\sigma+1}}{n}\mathbf{L}\xi. \tag{6.7}$$

Matrix $\mathbf{L}$ is the Laplacian of $K_{n,n}$

$$\mathbf{L} = \begin{pmatrix} nI_n & -J_n \\ -J_n & nI_n \end{pmatrix}, \tag{6.8}$$

where I_n is the $n \times n$ identity matrix and $J_n = \mathbf{1}_n\mathbf{1}_n^\mathsf{T}$. As a graph Laplacian of an undirected connected graph, $\mathbf{L}$ is a symmetric positive semidefinite matrix with a simple eigenvalue 0 [16]. Thus, the space homogeneous solution u^h is stable for $\sigma = 0$ and is unstable when $\sigma = 1$.[6] The linearization of (6.3) about u^s yields

$$\dot{\xi} = \frac{(-1)^{\sigma}}{n}\mathbf{L}\xi,$$

which, up to a sign, coincides with (6.7). Thus, u^s is unstable if $\sigma = 0$ and is stable for $\sigma = 1$.

The discrete model (6.3) has many other piecewise constant steady state solutions besides u^h and u^s. But the latter are the only two that approximate functions in $\tilde{C}(I)$, and, therefore, only these solutions can be attractors of the discrete system for large n (cf. Theorems 3.3, 5.2). This is consistent with the numerical simulations shown in Figure 6(b), (c). Numerical experiments show that the synchronous state is the attractor for the Kuramoto model with $\sigma = 0$, while the step function is the attractor for the model with $\sigma = 1$ (see Figure 6(b), (c)).

Remark 6.1. The Kuramoto model on the family of half-graphs (cf. Example 2.4) also exhibits stable step-like patterns, whose analysis follows the lines of that for the complete bipartite graphs.

In conclusion, we briefly discuss how the Kuramoto model on $\{K_{n,n}\}$ can be generalized to produce stable patterns with arbitrary number of steps. To this end, let $C_n = \langle V(C_n), E(G_n)\rangle$ be an n-cycle, i.e., $V(C_n) = [n]$ and $E(C_n) = \{(i,j) \in [n]^2 : \operatorname{dist}(i,j) = 1\}$. Recall $\operatorname{dist}(i,j) := \min\{|i-j|, n - |i-j|\}$. The adjacency matrix of C_n is given by

$$A(C_n) = \begin{pmatrix} 0 & 1 & 0 & \dots & 0 & 1 \\ 1 & 0 & 1 & \dots & 0 & 0 \\ & & & \dots & & \\ 1 & 0 & 0 & \dots & 1 & 0 \end{pmatrix}. \tag{6.9}$$

[6] The simple zero eigenvalue in the spectrum of the linearized problem reflects the translational invariance of (6.3), which does not affect the stability.

Copyright © by SIAM. Unauthorized reproduction of this article is prohibited.

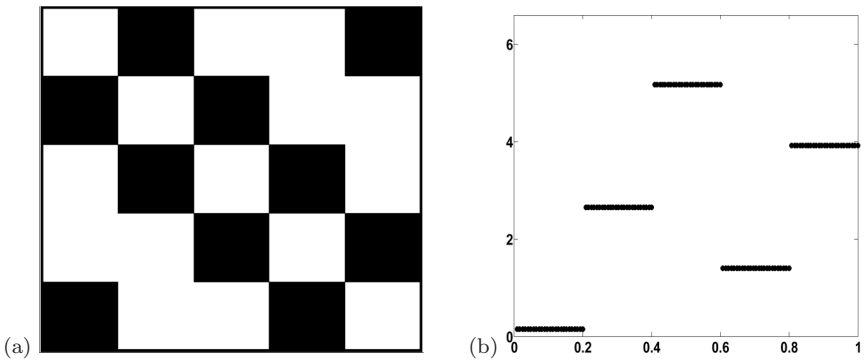

FIG. 7. (a) *The block structure of* $A(C_{n,m})$. (b) *A stable multistep pattern generated by the Kuramoto model on a multipartite graph.*

Let K_m denote the complete graph on m nodes. Define graph $C_{n,m} = C_n \otimes K_m$ on nm nodes by replacing each node of C_n with a copy of the complete graph K_m. The adjacency matrix of the resultant graph is the Kronecker product of $A(C_n)$ and $A(K_m)$

$$A(C_{n,m}) = A(C_n) \otimes A(K_m).$$

The block structure of $A(C_{n,m})$ is shown in Figure 7(a).

The Kuramoto model (6.3) with $K_{n,n}$ replaced by $C_{n,m}$ generates stable patterns with n steps like those shown in Figure 7(b). In computational neuroscience, such patterns have been sought in the context of modeling memory. The stability analysis of these multistep patterns can be done in analogy to the analysis in this subsection.

7. Conclusion. The heat equation is a fundamental equation of mathematical physics. On Euclidean domains, the heat operator is used to model phenomena involving diffusion, propagation, and pattern formation in diverse problems of physics and biology. On Riemannian manifolds, the heat equation has been a powerful tool for studying the topology of the underlying manifold [38]. Its discrete counterpart, the heat equation on graphs, plays an important role in the spectral graph theory [11].

Motivated by the dynamics of large networks, in this paper we have studied the nonlinear heat equation on dense graphs. We identified two classes of convergent graph sequences, for which the dynamics of large coupled networks is approximated by the heat equation on the graph limit. The latter is a nonlinear evolution equation with an integral operator that describes nonlocal spatial interactions. The nonlocal heat equation differs from its partial differential equation counterpart in several respects. First, the IVP for the heat equation on a graph limit is well-posed in both forward and backward time. Second, the solutions of the IVPs for the nonlocal heat equation lack the smoothening property, i.e., the spatial regularity of solutions for positive times is determined by the initial data and the regularity of the graph limit. In particular, the heat equation on a graph limit can have attractors that are piecewise continuous in space (see subsection 6.2), or combine regions with qualitatively distinct dynamics like in chimera states (see subsection 6.1).

Our analysis highlights the properties of the convergent graph sequences that allow taking the continuum limit for coupled dynamical systems. Note that for convergent sequences of simple graphs analyzed in section 4, we require that the graph

Downloaded 09/19/14 to 129.25.6.190. Redistribution subject to SIAM license or copyright; see http://www.siam.org/journals/ojsa.php

Copyright © by SIAM. Unauthorized reproduction of this article is prohibited.

Downloaded 09/19/14 to 129.25.6.190. Redistribution subject to SIAM license or copyright; see http://www.siam.org/journals/ojsa.php

limit is a $\{0,1\}$-valued graphon. For such sequences, we are able to represent the discrete problems using the step functions $\{W_{G_n}\}$ (cf. (2.3)), which converge to the limiting graphon W in the L^1-norm. This construction does not work for an arbitrary convergent sequence of simple graphs. For instance, a sequence of Paley graphs $\{P_n\}$ converges to Const $(1/2)$, the constant graphon equal to $1/2$ [8]. The corresponding sequence of step functions $\{W_{P_n}\}$ converges to Const $(1/2)$ in the cut-norm, but not in the L^1-norm. Thus, the results of this paper do not apply to dynamical networks on a sequence of Paley graphs. On the other hand, the analysis in [29] shows that the heat equation on the sequence of the Erdős–Rényi graphs (which is also a sequence of simple albeit random graphs converging to Const$(1/2)$) has a well-defined continuum limit. In contrast to the present work, the analysis of the continuum limit in [29] relies on the central limit theorem.

Our results for networks on convergent sequences of simple graphs also reveal what structural properties of graphs affect the accuracy of the continuum limit. Specifically, the rate of convergence estimate in Theorem 4.1 shows that the accuracy of approximation of the solutions of the discrete problems by their continuous counterparts may depend on the regularity of the boundary of support of the graph limit. In particular, the convergence may slow down significantly if the Hausdorff dimension of the boundary is close to 2. It is interesting to compare this result with the rate of convergence estimate for random networks in [29]. For random networks, the speed of convergence is determined by the central limit theorem and is independent of the regularity of the underlying graphon.

The theory of graph limits provides a useful set of tools for studying dynamics of large networks [25]. On one hand, known graph limits for various convergent sequences like that of half graphs or Erdős–Rényi graphs suggest continuum limits for the corresponding networks. On the other hand, this rich theory offers many useful ideas and analytical results that can be applied to the analysis of dynamical networks. In this paper, we analyzed two families of networks on convergent sequences of deterministic graphs. In [29, 30] a similar approach is used to study networks on convergent sequences of random graphs. Therefore, the results of this paper and in [29] justify the continuum limit for a broad class of networks.

Acknowledgments. The author thanks A. Grinshpan and D. Kaliuzhnyi-Verbovetskyi for useful discussions and valuable comments on the manuscript.

REFERENCES

[1] D.M. Abrams and S.H. Strogatz, *Chimera states in a ring of nonlocally coupled oscillators*, Internat. J. Bifur. Chaos Appl. Sci. Engrg., 16 (2006), pp. 21–37.

[2] D.M. Abrams, H.A. Yaple, and R.J. Wiener, *Dynamics of social group competition: Modeling the decline of religious affiliation*, Phys. Rev. Lett., 107 (2011), 088701.

[3] M. Barahona and L.M. Pecora, *Synchronization in small-world systems*, Phys. Rev. Lett., 89 (2002), 054101.

[4] D.S. Bassett and E. Bullmore, *Small-world brain networks*, Neuroscientist, 12 (2006), pp. 512–523.

[5] R. Ben Yishai, D. Hansel, and H. Sompolinsky, *Traveling waves and processing of weakly tuned inputs in a cortical network module*, J. Comput. Neurosci., 4 (1997), pp. 55–77.

[6] N. Biggs, *Algebraic Graph Theory*, 2nd ed., Cambridge University Press, Cambridge, 1993.

[7] C. Borgs, J. Chayes, L. Lovász, V. Sós, and K. Vesztergombi, *Limits of randomly grown graph sequences*, European J. Combin., 32 (2011), pp. 985–999.

[8] C. Borgs, J.T. Chayes, L. Lovász, V.T. Sós, and K. Vesztergombi, *Convergent sequences of dense graphs.* I. *Subgraph frequencies, metric properties and testing*, Adv. Math., 219 (2008), pp. 1801–1851.

Copyright © by SIAM. Unauthorized reproduction of this article is prohibited.

[9] C. Borgs, J. Chayes, L. Lovász, V.T. Sós, B. Szegedy, and K. Vesztergombi, *Graph limits and parameter testing*, in Proceedings of the 38th Annual ACM Symposium on Theory of Computing, ACM, New York, 2006, pp. 261–270.
[10] P. Cherrier and A. Milani, *Linear and Quasilinear Evolution Equations in Hilbert Space*, AMS, Providence, RI, 2012.
[11] F.R.K. Chung, *Spectral Graph Theory*, AMS, Providence, RI, 1997.
[12] Y.L. Daleckii and M.G. Krein, *Stability of Solutions of Differential Equations in Banach Space*, Translations of Mathematical Monographs 43, AMS, Providence, RI, 1974.
[13] F. Dorfler and F. Bullo, *Synchronization and transient stability in power networks and non-uniform Kuramoto oscillators*, SIAM J. Control Optim., 50 (2012), pp. 1616–1642.
[14] L.C. Evans, *Partial Differential Equations*, AMS, Providence, RI, 2010.
[15] K. Falconer, *Fractal Geometry: Mathematical Foundations and Applications*, John Wiley & Sons, New York, 1997.
[16] M. Fiedler, *Algebraic connectivity of graphs*, Czechoslovak Math. J., 23 (1973), pp. 298–305.
[17] T. Girnyk, M. Hasler, and Y. Maistrenko, *Multistability of twisted states in non-locally coupled Kuramoto-type models*, Chaos, 22 (2012), 013114.
[18] Y. Kuramoto, *Chemical Oscillations, Waves, and Turbulence*, Springer, Berlin, 1984.
[19] Y. Kuramoto and D. Battogtokh, *Coexistence of coherence and incoherence in nonlocally coupled phase oscillators*, Nonlinear Phenom. Complex Syst., 5 (2002), pp. 380–385.
[20] C.R. Laing, *Chimera states in heterogeneous networks*, Chaos, 19 (2009), 013113.
[21] C.R. Laing and C.C. Chow, *Stationary bumps in networks of spiking neurons*, Neural Comput., 13 (2001), pp. 1473–1494.
[22] C.R. Laing, K. Rajendran, and I.G. Kevrekidis, *Chimeras in random non-complete networks of phase oscillators*, Chaos, 22 (2012), 013132.
[23] L. Larger, B. Penkovsky, and Y. Maistrenko, *Virtual chimera states for delayed-feedback systems*, Phys. Rev. Lett., 111 (2013), 054103.
[24] R.D. Li and T. Erneux, *Preferential instability in arrays of coupled lasers*, Phys. Rev. A, 46 (1992), pp. 4252–4260.
[25] L. Lovász, *Large Networks and Graph Limits*, AMS, Providence, RI, 2012.
[26] L. Lovász and B. Szegedy, *Limits of dense graph sequences*, J. Combin. Theory Ser. B, 96 (2006), pp. 933–957.
[27] L. Lovász and B. Szegedy, *Szemerédi's lemma for the analyst*, Geom. Funct. Anal. 17 (2007), pp. 252–270.
[28] G.S. Medvedev, *Stochastic stability of continuous time consensus protocols*, SIAM J. Control Optim., 50 (2012), pp. 1859–1885.
[29] G.S. Medvedev, *The nonlinear heat equation on W-random graphs*, Arch. Ration. Mech. Anal., 21 (2014), pp. 781–803.
[30] G.S. Medvedev, *Small-world networks of Kuramoto oscillators*, Phys. D, 266 (2014), pp. 13–22.
[31] G.S. Medvedev and S. Zhuravytska, *The geometry of spontaneous spiking in neuronal networks*, J. Nonlinear Sci., 22 (2012), pp. 689–725.
[32] I. Omelchenko, B. Riemenschneider, P. Hövel, Y. Maistrenko, and E. Schöll, *Transition from spatial coherence to incoherence in coupled chaotic systems*, Phys. Rev. E, 85 (2012), 026212.
[33] O.E. Omelchenko, *Coherence-incoherence patterns in a ring of non-locally coupled phase oscillators*, Nonlinearity, 26 (2013), p. 2469.
[34] O.E. Omelchenko, M. Wolfrum, S. Yanchuk, Y. Maistrenko, and O. Sudakov, *Stationary patterns of coherence and incoherence in two-dimensional arrays of non-locally-coupled phase oscillators*, Phys. Rev. E, 85 (2012), 036210.
[35] E. Ott and T.M. Antonsen, *Low dimensional behavior of large systems of globally coupled oscillators*, Chaos, 18 (2008), 037113.
[36] J.R. Phillips, H.S.J. van der Zant, J. White, and T.P. Orlando, *Influence of induced magnetic fields on the static properties of Josephson-junction arrays*, Phys. Rev. B, 47 (1993), pp. 5219–5229.
[37] O. Pikhurko, *An analytic approach to stability*, Discrete Math., 310 (2010), pp. 2951–2964.
[38] S. Rosenberg, *The Laplacian on a Riemannian Manifold: An Introduction to Analysis on Manifolds*, Cambridge University Press, Cambridge, 1997.
[39] S.H. Strogatz and J. Mirollo, *Stability of incoherence in a population of coupled oscillators*, J. Statist. Phys., 63 (1991), pp. 613–635.
[40] S.H. Strogatz, *From Kuramoto to Crawford: Exploring the onset of synchronization in populations of coupled oscillators*, Phys. D, 143 (2000), pp. 1–20.
[41] N.V. Swindale, *The model for the formation of ocular dominance stripes*, Proc. R. Soc. Lond. B, 208 (1980), pp. 243–264.

Downloaded 09/19/14 to 129.25.6.190. Redistribution subject to SIAM license or copyright; see http://www.siam.org/journals/ojsa.php

Copyright © by SIAM. Unauthorized reproduction of this article is prohibited.

[42] M.R. Tinsley, S. Nkomo, and K. Showalter, *Chimera and phase-cluster states in populations of coupled chemical oscillators*, Nature Phys., 8 (2012), pp. 662–665.
[43] D. Tanaka and Y. Kuramoto, *Complex Ginzburg-Landau equation with nonlocal coupling*, Phys. Rev. E, 68 (2003), 026219.
[44] S. Watanabe and S.H. Strogatz, *Constants of motion for superconducting Josephson arrays*, Phys. D, 74 (1994), pp. 197–253.
[45] D.J. Watts and S.H. Strogatz, *Collective dynamics of small-world networks*, Nature, 393 (1998), pp. 440–442.
[46] D.A. Wiley, S.H. Strogatz, and M. Girvan, *The size of the sync basin*, Chaos, 16 (2006), 015103.

Downloaded 09/19/14 to 129.25.6.190. Redistribution subject to SIAM license or copyright; see http://www.siam.org/journals/ojsa.php

Copyright © by SIAM. Unauthorized reproduction of this article is prohibited.